Analytical Methods

Accepted Manuscript

This article can be cited before page numbers have been issued, to do this please use: Y. Tian, W. Zhou, B. Yin and B. Ye, *Anal. Methods*, 2017, DOI: 10.1039/C7AY02096A.

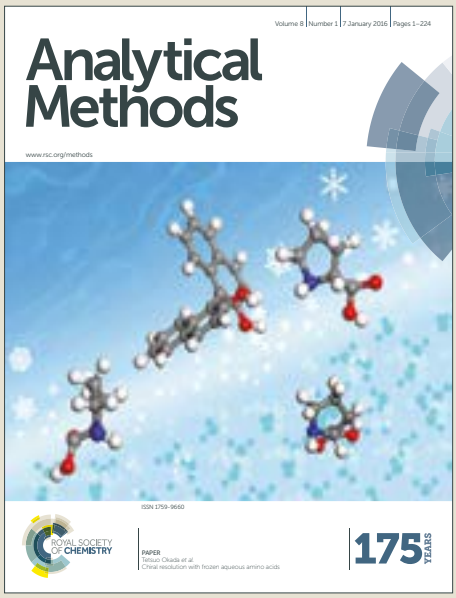

ROYAL SOCIETY OF CHEMISTRY

rsc.li/methods

View Article Online
DOI: 10.1039/C7AY02096A

Journal Name

ARTICLE

Highly sensitive surface-enhanced Raman scattering detection of adenosine triphosphate based on core-satellite assemblies

Received 00th January 20xx,
Accepted 00th January 20xx

DOI: 10.1039/x0xx00000x

www.rsc.org/

Ya-Fei Tian,[a] Wen Zhou,[a] Bin-Cheng Yin*[a] and Bang-Ce Ye[ab]

As an important small molecule, adenosine triphosphate (ATP) plays an important role in the regulation of cell metabolism and supplies energy for various biochemical reactions in organisms. We herein developed a sensitive surface-enhanced Raman scattering (SERS) biosensor for highly specific detection of ATP using core-satellite assemblies. To construct the aptamer-based biosensor, a known ATP binding aptamer was divided into two segments. The first thiol-labeled segment (DNA1) of the aptamer was immobilized on silver-coated gold nanostar (AuNS@Ag) surfaces by an Au-S bond. The second thiol-labeled segment (DNA2) was linked via an Au-S bond to gold nanoparticles (AuNPs), which were also decorated with a Raman active reporter molecule, 4-mercaptobenzoic acid (4-MBA). In the presence of ATP, DNA2 associated with DNA1, leading to greatly enhanced 4-MBA Raman intensity. The enhance Raman signal was linearly related to the logarithm of the ATP concentration in the range from 1 pM to 1 nM, with a detection limit of ~0.5 pM. In addition, the sensor featured an excellent selectivity to ATP over other interfering analogues of ATP (GTP, CTP, and UTP).

1. Introduction

Adenosine triphosphate (ATP) is an important small molecule in living organisms, and is an index of cell survival and cell injury.[1, 2] It is crucial in the regulation of cell metabolism and supplies energy for various biochemical reactions in organisms.[3] From this perspective, ATP levels can be used to evaluate cellular injury and proliferation induced by various small molecule drugs and biologics. Abnormal levels of ATP have been associated with specific diseases such as cardiovascular disease, which shows overproduction of ATP by creatine kinase.[4] In addition, ATP is often used as a microbial pollution index, in which the content of ATP reflects the degree of contamination.[5] The traditional ATP detection methods include electrophoresis,[6] high performance liquid chromatography (HPLC),[7] isotope tracing,[8] bioluminescence, and chemiluminescence.[9-11] In the determination of ATP by electrophoresis, the samples need to be separated by electrophoresis and then compared using an ultraviolet spectrophotometer, which needs complicated and time-consuming protocols.[12] HPLC is one of the widely used techniques for rapid analysis of different compounds at analytical levels with high efficiency, speed, and reproducibility.[13, 14] These two techniques are not sensitive enough to detect ATP with a low concentration. The isotope tracer method has the advantages of simplicity and sensitivity, but it requires use of radioactive materials.[15] Chemiluminescence and bioluminescence have high measurement accuracy, and can meet the requirements of different detection ranges, but the stability and specificity of the methods are problematic.[16] Therefore, it is of great significance to develop stable, specific, and sensitive ATP detection methods.

Recently, SERS has emerged as an ultra-rapid technique, allowing highly sensitive biological and chemical detection.[17, 18] A number of potential applications of SERS in medical research, food and drug safety, and environmental monitoring have been demonstrated.[19-21] Since the enhancement of SERS is mainly caused by chemical and electromagnetic enhancement,[22] metallic nanoparticles play a unique role in the fabrication of ultrasensitive biosensors. Localized surface plasmon resonance (LSPR) arises from resonant oscillations of the conducting electrons around the nanoparticles,[23, 24] SERS spectroscopy is therefore an invaluable tool for the detection of chemicals or DNA, even approaching the single molecule limit.[25-27] However, the SERS signal of a single encoded nanoparticle is too weak for wide application in ultrasensitive detection. Although aggregation can largely improve the SERS signal, uncontrollable aggregation results in signal heterogeneity with low reproducibility of the SERS assay.[28] Therefore, controllable nanoassemblies are critical for the preparation of SERS-active sensors.[29] Various controllable nanoassemblies have been fabricated, such as dimers,[30] trimers,[31] chains,[32] and pyramids.[33] In recent years, core-satellite assemblies have attracted great attention,[34-37] and

[a] Lab of Biosystem and Microanalysis, State Key Laboratory of Bioreactor Engineering, East China University of Science and Technology, Shanghai, 200237, China. Email: binchengyin@ecust.edu.cn
[b] School of Chemistry and Chemical Engineering, Shihezi University, Xinjiang, 832000, China
Electronic Supplementary Information (ESI) available: Details about Fig. S1-S8 and Table S1-S2. See DOI: 10.1039/x0xx00000x

View Article Online
DOI: 10.1039/C7AY02096A

SERS measurements have been reported by several groups, using both spherical nanoparticles and mixtures of spheres,[38-40] nanorods [41, 42] and nanostars[43, 44]. However, so far, the use of AuNS@Ag core-AuNP satellite assemblies has not been reported. As one of the best geometries, dispersed nanostars produce very strong SERS,[45, 46] due to their multiple sharp branches, the tips of which can produce strong electromagnetic field effects.[47] AuNS@Ag is a new hybrid bimetallic nanostar substrate that exhibits excellent SERS properties.[48] Compared to the uncoated AuNS, AuNS@Ag has been shown to provide more than an order-of-magnitude signal enhancement, making them excellent SERS substrates. The structure couples the plasmons focused on the multi-sharp tips, producing many "hotspots" that enhance the electromagnetic field around the particle.[49]

In the present work, we developed SERS-based biosensor for quantitative detection of ATP based on core-satellite assemblies. We fabricated silver-coated AuNS as the core to assemble with AuNP labeled with a Raman active reporter molecule to form AuNS@Ag core-AuNP satellite assemblies as SERS substrates. A well-known ATP binding aptamer was split into two segments. The first thiol-labeled segment of the aptamer was immobilized on the AuNS@Ag surfaces by the formation of an Au-S bond. The second segment was linked to AuNP, which was also decorated with Raman reporter molecules, 4-mercaptobenzoic acid (4-MBA). Following the addition of ATP, these two segments bound the ATP, resulting in AuNP assembly on the surfaces of the AuNS@Ag. The SERS intensity had a direct relationship with the number of AuNP satellite around the AuNS@Ag core. The experimental results showed that the SERS sensor has a limit of detection (LOD) down to ~0.5 pM with a linear range from 1 pM to 1 nM. Moreover, we showed that the sensor exhibits excellent selectivity to ATP over other interfering analogues of ATP, and allows practical application for quantitative ATP detection in 20% human serum samples.

2. Experimental section

2.1 Reagents and Materials

Thiolated DNA oligonucleotides (DNA1: 5'-SH-$(CH_2)_6$-TTTTTTA CCTGGGGGAGTAT-3'; DNA2: 5'-SH-$(CH_2)_6$-TTTTTTTGCGGA GGAAGGT-3') were manufactured by Shanghai Sangon Biological Engineering Technology & Services Co. Ltd. (Shanghai, China). Hydrogen tetrachloroaurate trihydrate ($HAuCl_4 \cdot 3H_2O$), sodium citrate tribasic dihydrate ($C_6H_5Na_3O_7 \cdot 2H_2O$), silver nitrate ($AgNO_3$), L-ascorbic acid (AA), sodium dodecyl sulfate (SDS), ammonium hydroxide (NH_4OH), tris(2-carboxyethy1)phosphine (TCEP), 4-mercaptobenzoic acid (4-MBA) were purchased from Sinopharm Chemical Reagent Co. Ltd (Shanghai, China). Adenosine triphosphate (ATP), guanosine triphosphate (GTP), cytidine triphosphate (CTP), and uridine triphosphate (UTP) were purchased from Sigma-Aldrich. Adenosine monophosphate (AMP) and adenosine diphosphate (ADP) were purchased from Adamas Reagent Co. Ltd. (Shanghai, China). Human serum and urine samples were collected from Shanghai Changzheng Hospital. Written informed consent was obtained from all study participants prior to enrollment, and the study was ap-proved by the ethics committees from the institution involved. The solutions were prepared using distilled water purified by a Milli-Q water purification system (Millipore Corp., Bedford, MA, USA) with an electrical resistance of 18.2 MΩ·cm. All glassware was cleaned with freshly prepared aqua regia and rinsed thoroughly with deionized water prior to preparation of nanoparticles.

2.2 Instrumentation

Ultraviolet-visible (UV-vis) absorption spectra were recorded with a multi-detection microplate reader (Bio-Tek, Winooski, USA) using a transparent 384-well microplate. To demonstrate the overall uniformity and morphology of the particles, the samples were examined by transmission electron microscopy (TEM, JEM-1400) and high-resolution transmission electron microscopy (HRTEM, JEM-2100). The samples for the TEM measurements were suspended in ethanol and supported on Cu grids. The size distribution of the nanoparticles were measured using a Zetasizer Nano ZS system (Malvern). A 633 nm laser was used for the dynamic light scattering (DLS) characterization. Raman spectra were collected on a portable Raman spectrometer (B&W Tek Instruments, USA) equipped with a 785 nm laser, a charge-coupled device (CCD) detector and a 40× objective lens with numerical aperture (NA) 0.65. The acquisition and analysis of Raman data were performed using the BWSpec4 software.

2.3 Synthesis of AuNP

We synthesized AuNPs (13 nm) based on literature procedures.[50] In a 250 mL round bottomed flask equipped with a condenser, 100 mL of $HAuCl_4$ (1 mM) was brought to a rolling boil with vigorous stirring. Fifteen mL of sodium citrate tribasic dihydrate (1%) was rapidly added, and the color of the vortexed solution changed from light yellow to wine red. After boiling for 15 min, the heating device was removed and stirring was continued for an additional 15 min. The solution was cooled to room temperature, filtered with a 0.22 μm membrane filter and stored at 4 °C. The as-prepared AuNPs were used as seeds to prepare AuNSs.

2.4 Synthesis of AuNS@Ag

First, two sizes of AuNSs (50 nm and 60 nm) were synthesized by a seed-mediated growth method with minor modification.[47] For AuNS synthesis, 200 μL of the above citrate-stabilized AuNP seed solution (6 nM) was added to 20 mL of 0.25 mM $HAuCl_4$ solution (with 20 μL of 1 M HCl) in a 50 mL centrifuge tube at room temperature. Quickly, 200 μL of $AgNO_3$ (1, 2 mM; 1 mM for 50 nm AuNS and 2 mM for 60 nm AuNS) and 100 μL of AA (0.1 M) were added simultaneously. The solution was stirred for 30 s as its color rapidly turned from light red to greenish-black. Then, 200 μL of SDS (2%) was added to the AuNS solution, which was left stirring for 5 min. The particles were then centrifuged at 1300 g for 15 min. The

View Article Online
DOI: 10.1039/C7AY02096A

supernatant was removed and the particles were redispersed in 20 mL of distilled water, and kept at 4 °C for the synthesis of AuNS@Ag according to previous literature.[48] Briefly, a 20 mL aliquot of the washed 50 nm or 60 nm AuNS seed solution (0.2 nM) was transferred into a 50 mL centrifuge tube. Subsequently, 100 μL of $AgNO_3$ (0.1 M) and an equivalent volume of AA (0.1 M) were added to the solution. The reduction of $AgNO_3$ by AA was initiated by the addition of NH_4OH (40 μL, 29%), and the color of the solution began to darken. About 5 min later, the solution color was stable, indicating that the reaction was complete. Then solution was centrifuged at 1000 g for 15 min. Then, the precipitate was collected and redispersed in water for further use.

2.5 Fabrication of ssDNA-functionalized AuNS@Ag and AuNP

First, 200 μL of DNA1 and DNA2 were added to a 1.5 mL centrifuge tube, respectively. Ten μL of freshly prepared TCEP (10 mM) was added to the centrifuge tube to activate the thiol-modified DNA1 and DNA2. The DNA1 and DNA2 were incubated at room temperature for 2 h, respectively. AuNS@Ag were modified with DNA1 at a molar ratio of 500:1. Briefly, DNA1 (10 μL, 10 μM) was added to the as-prepared AuNS@Ag solution (200 μL, 1 nM) and incubated for 3 h at room temperature. Subsequently, NaCl (10 μL, 0. 5 M) was added and then the mixture was incubated for 8 h with constant shaking. The excess DNA1 was removed by three centrifugations at 1000 g for 10 min. The precipitate was resuspended in 200 μL of PB buffer. The mixture was denoted as AuNS@Ag-DNA1.

AuNPs were modified with the DNA2 at a molar ratio of 10:1. AuNPs were resuspended in water at a final concentration of 10 nM by centrifugation. DNA2 (2 μL, 10 μM) was added to the AuNP solution (200 μL, 10 nM) under vigorous stirring. The Raman label (4-MBA) solution was then added at a final concentration of 10 μM. After incubation at 37 °C for 8 h, the solution ws centrifuged at 8000 g for 15 min. The particles were washed three times with PB buffer. The precipitate, denoted as 4-MBA-modified-AuNP-DNA2, was collected and resuspended in 200 μL of PB buffer.

2.6 SERS detection of ATP

For detection of ATP, various concentrations of ATP were prepared using serial dilution of the ATP stock solution (10^{-2} M). Briefly, 200 μL of ATP at a series of different concentrations was mixed with 40 μL of the prepared AuNS@Ag-DNA1 (1 nM) and 200 μL of the prepared 4-MBA-modified AuNP-DNA2 (10 nM) with gentle shaking. The solution was then incubated at 37 °C for 4 h. The AuNP-DNA2 without assembly were removed by centrifugation (three times) at 1000 g for 10 min. Then, the supernatant was removed to give a residual volume of 10 μL. Afterwards, 10 μL of the residual AuNS@Ag-AuNP solution was deposited on a cleaned silica slide for further SERS measurement.

3. Results and discussion

3.1 Synthesis of AuNS@Ag and SERS sensing strategy for ATP detection

A multi-step protocol for AuNS@Ag fabrication and the working principle of ATP detection based on satellite assemblies are shown in Scheme 1. Schematically, the AuNP is prepared via the classical citrate reduction method and used as a seed for AuNS fabrication using a Au seed-mediated growth method, in which the Au seed is used for the growth of a silver shell, with AA as the reducing agent and $AgNO_3$ as the precursor to elemental silver. AuNS@Ag is fabricated by adding $AgNO_3$ and AA to the prepared AuNS solution, and NH_4OH is introduced to increase the pH, initiating the reduction of Ag^+ to Ag^0 by AA with a color change of the solution. An ATP binding aptamer is split into two segments (DNA1 and DNA2), which are modified with thiol moieties and poly T spacers. DNA1 and DNA2 are immobilized on the surfaces of AuNS@Ag and AuNPs by the formation of Au-S bonds, respectively. The Raman reporters (4-MBA) are also labeled on the AuNP surfaces via Au-S bonds. In the presence of ATP, the two ssDNA segments reassemble into the intact aptamer structure and then induce the formation of AuNS@Ag core-AuNP satellite assemblies. Between AuNS@Ag core and AuNP satellite can form short gap distances, the more the conjunction regions, the greater number of "hotspots" is formed. In this manner, the coupled plasmons can enhance the intensity of the electromagnetic field over a wide connection area, resulting in an enormous enhancement of SERS intensity. The assembly degree of AuNS@Ag core-AuNP satellite reflects the concentration of ATP, while the SERS signal depends on the assembly degree of AuNS@Ag core-AuNP satellite assemblies. Therefore, the amount of ATP present can be quantitatively determined by the SERS signal.

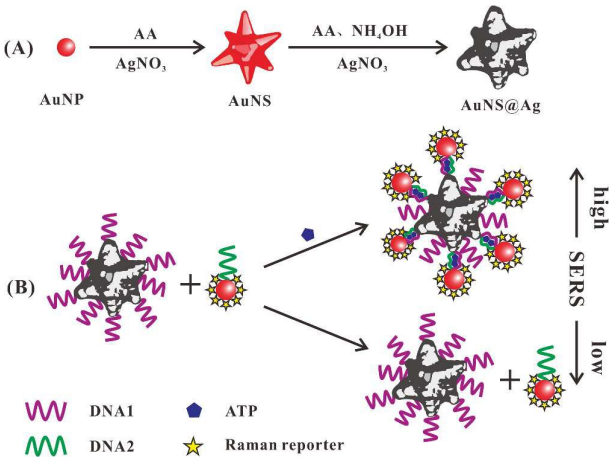

Scheme 1 Schematic representation of the fabrication of AuNS@Ag (A) and SERS sensing strategy for ATP detection (B).

3.2 Characterization of AuNS@Ag

To investigate the Raman enhancement effect of the various silver coatings, two sizes of AuNS (50 nm and 60 nm) were as seeds for the preparation of AuNS@Ag with different Ag shell thicknesses (see the Supporting Information for the experimet). The AuNS@Ag samples were labeled with 4-MBA for SERS measurements. Fig. 1A

View Article Online
DOI: 10.1039/C7AY02096A

showed the integrated, background-subtracted SERS intensity of 50 nm and 60 nm AuNSs with various amounts of silver at 1078 cm^{-1} and the corresponding SERS spectra were shown in Fig. S1. It was observed that using 50 nm AuNSs as seeds, the highest intensity was obtained when adding 4 mL of $AgNO_3$ (0.1 M). While, the highest intensity of 60 nm AuNSs as seeds was obtained when adding 5 mL of $AgNO_3$ (0.1 M). By comparing their highest intensities, we chose 60 nm AuNSs as seeds, and the amount of 5 mL $AgNO_3$ (0.1 M) for the AuNS@Ag fabrication. In addition, it was clearly observed that a higher amount of silver does not lead to higher SERS response.

The AuNS@Ag at various stages of the synthesis process was characterized using UV-vis absorption spectra (Fig. 1B). Compared with the absorption peaks of AuNPs (blue curve) located at 520 nm and 60 nm AuNS (green curve) located at 735 nm, the absorption peak of AuNS@Ag blue-shift, indicating Ag successfully coated 60 nm AuNS. The size distributions of the nanoparticles were measured by DLS (Fig. S2). DLS analysis showed size of 13±1.1, 60±3.4 and 68±2.2 nm for AuNP, 60 nm AuNS and AuNS@Ag, respectively. AuNS displayed a well-defined star-shaped structure as shown TEM image (Fig. S3). The preparation of uniform AuNS@Ag were critical for the generation of a stable SERS signal. As shown in Fig. 1C, HRTEM image clearly demonstrated the detailed structures of branched AuNS@Ag. Moreover, the colors and SERS spectra of the prepared nanoparticles were characterized (Fig. S4). To further confirm the formation of AuNS@Ag composite, samples were analyzed by electron mapping image analysis. The different color areas shown in parts Fig. 1D indicate Au and Ag-enriched areas of the sample, respectively, which indicate the presence of Ag in the outer surface of the AuNS.

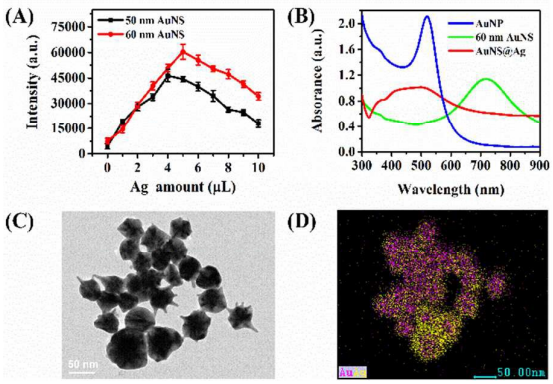

Fig. 1 (A) SERS intensity at 1078 cm^{-1} for AuNS@Ag samples (50 nm and 60 nm AuNS as seeds) with various amounts of silver coating. SERS detection parameters: $\lambda_{excitation}$ = 785 nm, accumulation time = 10 s, laser power = 50 mW. (B) UV-visible spectra of the 13 nm AuNP, 60 nm AuNS, and corresponding AuNS@Ag. (C) HRTEM image of AuNS@Ag. (D) Elemental mapping of the AuNS@Ag composite.

3.3 Investigation of the feasibility

We used 4-MBA as Raman reporter to investigate the feasibility of proposed sensor for ATP detection. As shown in Fig. 2, in the absence of 4-MBA, no SERS signals were observed (curve a,b). In the presence of 4-MBA, while ATP was absent, 4-MBA-modified AuNP-DNA2 weren't able to combined with AuNS@Ag-DNA1, so it couldn't be assembled into a core-satellite structure, which was demonstrated by no apparent SERS signal (curve c). In the presence of 4-MBA and ATP (100 pM, 1 nM), 4-MBA-modified AuNP-DNA2 and AuNS@Ag-DNA1 assembled into a core-satellite structure with lots of short gaps, which was demonstrated by obvious SERS signal (curve d, e). By comparing the intensity of SERS signals, we confirmed that the indirect SERS sensing method using 4-MBA as a Raman reporter was feasible for ATP analysis. In addition, the assembled AuNS@Ag core-AuNP satellites in the presence of different concentrations of ATP were clearly observed under TEM (Fig. 2B-D). It is showed that no AuNP was assembled around AuNS in the absence of ATP, and more amount of AuNP was assembled around AuNS with higher concentration of ATP. These TEM images provided the direct evidence of ATP-assisted assembly degree of AuNS@Ag core-AuNP satellite.

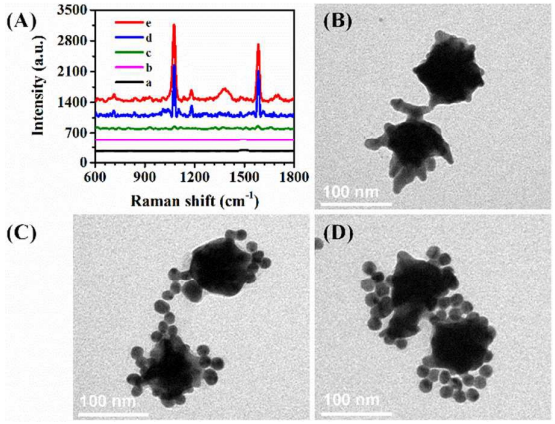

Fig. 2 (A) SERS spectra corresponding to (a) 4-MBA-unmodified AuNP-DNA2 and AuNS@Ag-DNA1 in the absence of ATP, (b) 4-MBA-unmodified AuNP-DNA2 and AuNS@Ag-DNA1 in the presence of 100 pM ATP, (c) 4-MBA-modified AuNP-DNA2 and AuNS@Ag-DNA1 in the absence of ATP, 4-MBA-modified AuNP-DNA2 and AuNS@Ag-DNA1 in the presence of 100 pM (d) and 1 nM ATP (e). TEM images of AuNS@Ag-AuNP assemblies in the presence of different concentrations of ATP: 0 pM (B); 100 pM (C); 1 nM (D).

3.4 Sensitivity investigation

For quantatitve ATP detection, eight ATP standards were added to the system containing AuNS@Ag-DNA1 and 4-MBA-modified AuNP-DNA2 at final ATP concentrations of 0, 1, 5, 10, 50, 100, 500, and 1000 pM, respectively. The SERS spectra of 4-MBA produced from AuNS@Ag core-AuNP satellite assemblies with different concentrations of ATP were recorded. As shown in Fig. 3A, pronounced SERS bands of 4-MBA at 524, 717, 845, 1011, 1078, 1144, 1178, 1412, 1480 and 1588 cm^{-1} were unambiguously observed in the presence of ATP. We chose the characteristic 4-MBA peak at 1078 cm^{-1} to quantitatively analyze ATP. The increase of SERS intensity as a function of ATP concentration indicated that the number of AuNS@Ag core-AuNP satellite assemblies increased with increasing concentration of ATP. Fig. 3B showed that the intensity of

View Article Online
DOI: 10.1039/C7AY02096A

the 1078 cm^{-1} peak increased as the concentration of ATP increased, and a standard curve was obtained for the SERS intensity against the logarithm of the ATP concentration over the range of 1 pM to 1 nM. The curve exhibited a good linear relationship (R^2 = 0.994), and the limit of detection (LOD) based on a signal-to-noise ratio of three was estimated to be ~0.5 pM. As shown in Table S1, our SERS sensor provided a high sensitivity for ATP detection compared to the reported methods. To futher study the application of the SERS sensor, biological sample of 20% human serum was employed. After pretreatment of the human serum samples, ATP standard solutions were added at a final concentrations of 1000, 500, and 100 pM. As shown in Table S2, the recovery of ATP ranged from 89.5% to 103.3%, and the results obtained by our sensor were highly consistent with ATP bioluminescent assay kit (Fig. S5). We further applied our method to detect ATP in biological sample of human urine (Fig. S6, Table S3).

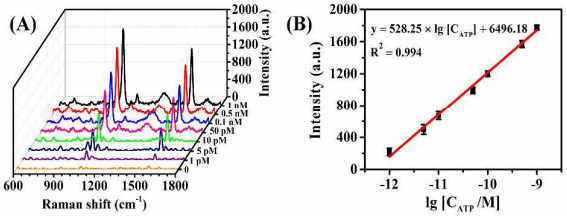

Fig. 3 (A) SERS spectra of 4-MBA for quantitative evaluation of the ATP with different concentrations. (B) The standard curve based on the 1078 cm^{-1} peak of 4-MBA. The Raman intensity shows a linear relationship with the logarithm of the ATP concentration from 1 pM to 1 nM (R^2 = 0.994). The error bars represent standard deviations based on three independent measurements. SERS detection parameters: $\lambda_{excitation}$ = 785 nm, accumulation time = 10 s, laser power = 100 mW.

3.5 Reproducibility and stability investigation

In addition to the high sensitivity, the AuNS@Ag core-AuNP satellite assemblies provided reproducible SERS signals. The SERS spectra of 4-MBA produced from 10 random spots (within an area of 60 μm^2) with 50 pM of ATP were recorded (Fig. S7A). The SERS intensities were comparable, suggesting that the surfaces of the SERS assemblies provided uniform SERS enhancements. Additionally, we compared the SERS intensities of the characteristic 1078 cm^{-1} line of 4-MBA in these 10 spectra (Fig. S7B). The SERS signal variations were less than 5.6%, suggesting excellent reproducibility of the SERS signals enhanced by the AuNS@Ag core-AuNP satellite assemblies. In addition, the stability of the sensors was investigated within 24 h and 7 days, respectively. We prepared 11 sensors of the same batch, and then applied for the detection of 50 pM ATP as model at different time points (Fig. S8). The results revealed that the SERS intensities could maintain 98.1% and 94.8% of the initial SERS intensity after 24 h and 7 days, respectively, indicating a good stability.

3.6 Specificity of the sensor for ATP

In order to investigate the specificity of the SERS sensor for ATP detection, ATP analogues were examined by parallel experiments, including GTP, CTP, and UTP at a concentration of 100 nM. As shown in Fig. 4A, only feeble SERS signals were observed for ATP analogues other than ATP due to their low binding affinity to the aptamer, while significant SERS enhancement was obtained with the addition of 1 nM ATP, showing excellent specificity of the SERS sensors for ATP detection. For a more direct quantitative comparison, corresponding SERS intensities of the 1078 cm^{-1} peak of 4-MBA in the presence of ATP and ATP analogues are represented in a bar graph in Fig. 4B. It should be noted that our sensor could not differentiate ATP from AMP and ADP (Fig. S9), because ATP aptamer has the same affinity toward ATP, ADP, and AMP.

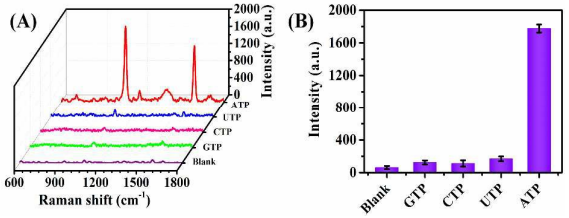

Fig. 4 (A) Selectivity of the SERS method for 1 nM ATP and 100 nM ATP analogs (GTP, CTP and UTP). (B) The SERS intensity of the 1078 cm^{-1} peak was utilized for comparison. The error bars represent standard deviations based on three independent measurements. SERS detection parameters: $\lambda_{excitation}$ = 785 nm, accumulation time = 10 s, laser power = 100 mW.

4. Conclusions

In summary, we have proposed a sensitive SERS method for highly specific detection of ATP, based on the use of unique AuNS@Ag core-AuNP satellite nanoassemblies. The presence of ATP induces the assembly of AuNS@Ag and AuNPs through the specific recognition of ATP by the aptamer. The SERS sensor has high sensitivity and specificity for ATP over its other analogues (GTP, CTP, and UTP). Since the SERS sensor is easily fabricated, we believe that it has potential for a wide variety of applications.

Conflicts of interest

The authors declare no competing financial interest.

Acknowledgements

This work was jointly supported by the National Natural Science Foundation of China (Grants 21675052, 21335003, 21575089), and the Fundamental Research Funds for the Central Universities.

References

1 H. J. Agteresch, P. C. Dagnelie and J. W. van den Berg, *Drugs*, 1999, **58**, 211-232.
2 F. Yu, L. Li and F. Chen, *Anal. Chim. Acta*, 2008, **610**, 257-262.
3 T. Tatsumi, J. Shiraishi, N. Keira, K. Akashi, A. Mano, S. Yamanaka, S. Matoba, S. Fushiki, H. Fliss and M. Nakagawa, *Cardiovasc. Res.*, 2003, **59**, 428-440.

View Article Online
DOI: 10.1039/C7AY02096A

4 J. F. Callan, R. C. Mulrooney and S. Kamila, *J Fluoresc*, 2008, **18**, 1157-1161.
5 Y. Wei, Y. Chen, H. Li, S. Shuang, C. Dong and G. Wang, *Biosens. Bioelectron.*, 2015, **63**, 311-316.
6 P. M. Yangyuoru, S. Dhakal, Z. Yu, D. Koirala, S. M. Mwongela, H. Mao and A. Chem, *Anal. Chem.*, 2012, **84**, 5298-5303.
7 L. Du, Y. Zhang, Y. Du, D. Yang, F. Gao and D. Tang, *Rsc Adv*, 2015, **5**, 100960-100967.
8 M. Scian, M. Acchione, M. Li and W. M. Atkins, *Biochemistry*, 2014, **53**, 991-1000.
9 B. F. Liu, M. Ozaki, H. Hisamoto, Q. Luo, Y. Utsumi, T. Hattori and S. Terabe, *Anal. Chem.*, 2005, **77**, 573-578.
10 S. Zhang, Y. Yan and S. Bi, *Anal. Chem.*, 2009, **81**, 8695-8701.
11 Y. Song, X. Yang, Z. Li, Y. Zhao and A. Fan, *Biosens. Bioelectron.*, 2014, **51**, 232-237.
12 J. Kamarýt, M. Muchová and J. Stejskal, *Eur. J. Clin. Chem. Clin. Biochem*, 1996, **34**, 969-973.
13 M. Michaud, E. Jourdan, C. Ravelet, A. Villet, A. Ravel, C. Grosset and E. Peyrin, *Anal. Chem.*, 2004, **76**, 1015-1020.
14 X. Xue, F. Wang, J. Zhou, F. Chen, Y. Li and J. Zhao, *J. Agric. Food Chem.*, 2009, **57**, 4500-4505.
15 X. Li, C. C. Wong, Z. Tang, J. Wu, S. Li, Y. Qian, J. Xu, Z. Yang, Y. Shen and J. Yu, *Talanta*, 2017, **162**, 285-292.
16 A. Roda, P. Pasini, M. Mirasoli, E. Michelini and M. Guardigli, *Trends Biotechnol.*, 2004, **22**, 295-303.
17 R. Zhang, Y. Zhang, Z. C. Dong, S. Jiang, C. Zhang, L. G. Chen, L. Zhang, Y. Liao, J. Aizpurua and Y. Luo, *Nature*, 2013, **498**, 82-86.
18 Y. Wang, B. Yan and L. Chen, *Chem. Rev.*, 2012, **113**, 1391-1428.
19 R. Perez-Pineiro, M. A. Correa-Duarte, V. Salgueirino and R. A. Alvarez-Puebla, *Nanoscale*, 2012, **4**, 113-116.
20 Y. Zhou, J. Chen, L. Zhang and L. Yang, *Eur. J. Inorg. Chem.*, 2012, **2012**, 3176-3182.
21 Y. Xie, Y. Li, L. Niu, H. Wang, H. Qian and W. Yao, *Talanta*, 2012, **100**, 32-37.
22 D. Graham, G. Mcanally, J. C. Jones and W. E. Smith, *Chem. Commun.*, 1998, **11**, 1187-1188.
23 L. Xu, H. Kuang, L. Wang and C. Xu, *J. Mater. Chem.*, 2011, **21**, 16759-16782.
24 S. K. Dondapati, T. K. Sau, C. Hrelescu, T. A. Klar, F. D. Stefani and J. Feldmann, *ACS Nano*, 2010, **4**, 6318-6322.
25 Y. C. Cao, R. Jin and C. A. Mirkin, *Science*, 2002, **297**, 1536-1540.
26 P. Monica, B. Monica, F. Cosmin and A. Simion, *Nanotechnology*, 2012, **23**, 055501.
27 C. G. Artur, R. Miller, M. Meyer, E. C. L. Ru and P. G. Etchegoin, *Phys. Chem. Chem. Phys.*, 2012, **14**, 3219-3225.
28 S. Schlücker, *Angew. Chem. Int. Ed.*, 2014, **53**, 4756-4795.
29 K. Liu, N. Zhao and E. Kumacheva, *Chem. Soc. Rev.*, 2011, **40**, 656-671.
30 F. J. Timmermans, A. T. M. Lenferink, H. A. G. M. van Wolferen and C. Otto, *Analyst*, 2016, **141**, 6455-6462.
31 Y. Zheng, T. Thai, P. Reineck, L. Qiu, Y. Guo and U. Bach, *Adv. Funct. Mater.*, 2013, **23**, 1519-1526.
32 W. Ma, H. Kuang, L. Xu, L. Ding, C. Xu, L. Wang and N. A. Kotov, *Nat. Commun.*, 2013, **4**, 2689-2696.
33 L. Xu, W. Yan, W. Ma, H. Kuang, X. Wu, L. Liu, Y. Zhao, L. Wang and C. Xu, *Adv. Mater.*, 2015, **27**, 1706-1711.
34 J. Feng, X. Wu, W. Ma, H. Kuang, L. Xu and C. Xu, *Chem. Commun.*, 2015, **51**, 14761-14763.
35 D. S. I. As, R. Thomas and L. Fabris, *Phys.Chem. Chem.Phys.*, 2015, **17**, 21133-21142.
36 J. Prasad, I. Zins, R. Branscheid, J. Becker, A. H. R. Koch, G. Fytas, U. Kolb and C. Sönnichsen, *J. Phys. Chem.C*, 2015, **119**, 5577-5582.
37 J. H. Yoon, J. Lim and S. Yoon, *Acs Nano*, 2012, **6**, 7199-7208.
38 N. H. Kim, S. J. Lee and M. Moskovits, *Adv. mater*, 2011, **23**, 4152-4156.
39 S. Y. Chen and A. A. Lazarides, *J. Phys. Chem. C*, 2009, **113**, 12167-12175.
40 N. Gandra, A. Abbas, L. Tian and S. Singamaneni, *Nano Lett.*, 2012, **12**, 2645-2651.
41 L. Xu, H. Kuang, C. Xu, W. Ma, L. Wang and N. A. Kotov, *J. Am. Chem. Soc.*, 2012, **134**, 1699-1709.
42 Y. Wang, K. Lee and J. Irudayaraj, *Chem. Commun.*, 2010, **46**, 613-615.
43 A. S. Indrasekara, R. Thomas and L. Fabris, *Phys. Chem. Chem. Phys.*, 2015, **17**, 21133-21142.
44 A. Li, L. Tang, D. Song, S. Song, W. Ma, L. Xu, H. Kuang, X. Wu, L. Liu and X. Chen, *Nanoscale*, 2016, **8**, 1873-1878.
45 G. Lu, T. Z. Forbes and A. J. Haes, *Analyst*, 2016, **141**, 5137-5143.
46 T. Yang and J. Jiang, *Small*, 2016, **12**, 4980-4985.
47 H. Yuan, C. G. Khoury, H. Hwang, C. M. Wilson, G. A. Grant and T. Vo-Dinh, *Nanotechnology*, 2012, **23**, 075102.
48 A. M. Fales, H. Yuan and T. Vo-Dinh, *J. Phys. Chem. C*, 2014, **118**, 3708-3715.
49 C. Hrelescu, T. K. Sau, A. L. Rogach, F. Jäckel, G. Laurent, L. Douillard and F. Charra, *Nano Lett.*, 2011, **11**, 402-407.
50 K. C. Grabar, R. G. Freeman, M. B. Hommer and M. J. Natan, *Anal. Chem.*, 1995, **67**, 735-743.